



FET PET reveals considerable spatial differences in tumour burden compared to conventional MRI in newly diagnosed glioblastoma

Philipp Lohmann¹ · Pantelis Stavrinou² · Katharina Lipke¹ · Elena K. Bauer³ · Garry Ceccon³ · Jan-Michael Werner³ · Bernd Neumaier¹ · Gereon R. Fink^{1,3} · Nadim J. Shah^{1,4} · Karl-Josef Langen^{1,5} · Norbert Galldiks^{1,3,6}

Received: 31 July 2018 / Accepted: 3 October 2018 / Published online: 16 October 2018
© Springer-Verlag GmbH Germany, part of Springer Nature 2018

Abstract

Purpose Areas of contrast enhancement (CE) on MRI are usually the target for resection or radiotherapy target volume definition in glioblastomas. However, the solid tumour mass may extend beyond areas of CE. Amino acid PET can detect parts of the tumour that show no CE. We systematically investigated tumour volumes delineated by amino acid PET and MRI in patients with newly diagnosed, untreated glioblastoma.

Methods Preoperatively, 50 patients with neuropathologically confirmed glioblastoma underwent *O*-(2-[¹⁸F]-fluoroethyl)-L-tyrosine (FET) PET, and fluid-attenuated inversion recovery (FLAIR) and contrast-enhanced MRI. Areas of CE were manually segmented. FET PET tumour volumes were segmented using a tumour-to-brain ratio of ≥ 1.6 . The percentage overlap volumes, and Dice and Jaccard spatial similarity coefficients (DSC, JSC) were calculated. FLAIR images were evaluated visually.

Results In 43 patients (86%), the FET tumour volume was significantly larger than the CE volume (21.5 ± 14.3 mL vs. 9.4 ± 11.3 mL; $P < 0.001$). Forty patients (80%) showed both increased uptake of FET and CE. In these 40 patients, the spatial similarity between FET uptake and CE was low (mean DSC 0.39 ± 0.21 , mean JSC 0.26 ± 0.16). Ten patients (20%) showed no CE, and one of these patients showed no FET uptake. In five patients (10%), increased FET uptake was present outside areas of FLAIR hyperintensity.

Conclusion Our results show that the metabolically active tumour volume delineated by FET PET is significantly larger than tumour volume delineated by CE. Furthermore, the results strongly suggest that the information derived from both imaging modalities should be integrated into the management of patients with newly diagnosed glioblastoma.

Keywords FET PET tumour volume · Volumetry · Amino acid PET · MRI contrast enhancement · FLAIR hyperintensity · Target volume definition

Introduction

Despite significant advances in diagnostics and therapy over the last decades, the prognosis for patients with glioblastoma (GBM), the most frequent form of glioma and the most aggressive and lethal primary brain tumour, remains dismal (median survival 15–20 months) [1–3]. Currently, the proposed first-line therapy for patients with GBM is a maximally safe resection followed by radiotherapy plus concomitant and adjuvant temozolomide chemotherapy [1, 4]. Importantly, the extent of the tumour resection is associated with improved overall survival, i.e. a “complete” resection (currently defined as a lack of contrast enhancement on the early postoperative MRI within 24–48 h of surgery [5]) is superior to resection smaller than the area of contrast enhancement or biopsy only [6–8]. Consequently, contrast-enhancing tumour portions on MRI are the target of

✉ Philipp Lohmann
p.lohmann@fz-juelich.de

¹ Institute of Neuroscience and Medicine (INM-3, -4, -5), Forschungszentrum Juelich, 52425 Juelich, Germany

² Department of Neurosurgery, University of Cologne, Cologne, Germany

³ Department of Neurology, University of Cologne, Cologne, Germany

⁴ Department of Neurology, University Hospital RWTH Aachen, Aachen, Germany

⁵ Department of Nuclear Medicine, University Hospital RWTH Aachen, Aachen, Germany

⁶ Center of Integrated Oncology (CIO), Universities of Cologne and Bonn, Cologne, Germany

neurosurgical resection in the majority of patients [4, 9]. Similar to neurosurgical resection planning, radiotherapy target volume definition is also often based on contrast-enhanced MRI [10]. In stark contrast, several studies have revealed that a considerable number of glioma cells, or even the main tumour burden, may not show contrast enhancement, particularly in patients with GBM [11–13]. Furthermore, comparison of the histopathological findings in whole-brain sections from patients with brain tumours with MRI data has shown that the extent of malignant gliomas is not correctly delineated by conventional MRI [14]. Finally, the precise delineation of glioma tissue is particularly problematic if no contrast enhancement is present, as is frequently observed in low-grade gliomas, and even 30–40% of anaplastic gliomas show no contrast enhancement [15]. In rare cases, this also occurs in patients with GBM [16, 17]. In such patients, the hyperintensity on T2-weighted or fluid-attenuated inversion recovery (FLAIR) MRI is frequently used for treatment planning [18].

Over the past years, several studies have shown that PET using radiolabelled amino acids detects tumour parts that show no contrast enhancement and provides better delineation of gliomas before treatment planning [19–22]. A number of amino acid PET studies using L-methyl- ^{11}C -methionine (MET) or *O*-(2- ^{18}F)-fluoroethyl-L-tyrosine (FET) have evaluated the correlation between imaging findings and histology. The results suggest reliable detection of glioma tissue independent of the integrity of the blood–brain barrier [19, 23–25]. Consistent with these findings, a post-mortem study compared MET PET and contrast-enhanced CT findings with whole-brain histopathology in a patient with an anaplastic astrocytoma. MET PET was able to correctly identify the full tumour extent while contrast-enhanced CT missed more than 50% of the tumour mass [26].

To the best of our knowledge, the fraction of untreated GBM that shows significant differences between contrast enhancement, FLAIR hyperintensity and FET accumulation, and whether this is relevant in clinical practice, remains to be investigated. To this end, we performed a systematic volumetric comparison between FET uptake and MR contrast enhancement and a visual comparison with FLAIR hyperintensity in a series of 50 patients with newly diagnosed GBM in terms of tumour size, overlap, and spatial correlation.

Materials and methods

Patients

Between February 2010 and August 2017, 50 adult patients with a newly diagnosed and untreated GBM investigated using FET PET at the Institute of Neuroscience and Medicine, Forschungszentrum Juelich, Germany, were included in this retrospective study (19 women, 31 men; mean age $56 \pm$

14 years, range 26–79 years). Postoperatively, neuropathological work-up confirmed GBM in all patients. The study adhered to the standards established in the Declaration of Helsinki. All patients provided written informed consent before each FET PET investigation. Given its retrospective nature, the local ethics committee of the University of Aachen waived the requirement for additional approval. Table 1 presents further details of all patients.

MR imaging

Before neuropathological confirmation, all patients underwent a 3D T2-weighted FLAIR MRI scan and a 3D T1-weighted MRI scan after intravenous administration of gadoteric acid (0.1 mmol/kg body weight). Five patients were scanned using a 3 T Achieva MRI scanner (Philips Medical Systems, Inc.), 17 patients using a 1.5 T Intera MRI scanner (Philips Medical Systems, Inc.), and 28 patients using a high-resolution 3 T hybrid PET/MR scanner (3 T Tim TRIO; Siemens Medical Systems, Inc.). FLAIR images were not available or incomplete in four patients.

FET PET imaging

The amino acid FET was produced and used as described previously [27, 28]. Before neuropathological confirmation and close in time to the MRI examination, all patients underwent a dynamic PET scan from 0 to 50 min after injection of 3 MBq of FET per kg body weight. The time between MRI and PET was in the range 0–20 days (median 0 days). Fifteen patients were scanned using a stand-alone PET scanner (ECAT EXACT HR+, Siemens Medical Systems, Inc.) in 3D mode (32 rings, axial field of view 15.5 cm). The reconstructed dynamic dataset consisted of 16 time-frames (5×1 min, 5×3 min, 6×5 min). A transmission scan (duration 10 min) using three rotating line sources ($^{68}\text{Ge}/^{68}\text{Ga}$) was used for attenuation correction. Before reconstruction using the iterative ordered subsets expectation maximization (OSEM) algorithm (16 subsets, six iterations), data were corrected for dead time, random and scatter coincidences. The other 35 patients were scanned using a high-resolution 3 T hybrid PET/MR scanner (BrainPET, Siemens Medical Systems, Inc.; 72 rings, axial field of view 19.2 cm). Image data were corrected for random and scatter coincidences, as well as for dead time before ordinary Poisson OSEM reconstruction using software provided by the manufacturer (two subsets, 32 iterations). The reconstructed dynamic dataset consisted of 16 time-frames (5×1 min, 5×3 min, 6×5 min). Since the hybrid PET/MR scanner did not provide a transmission source, attenuation correction was performed by a template-based MRI approach [29].

Table 1 Demographic and clinical data of the patient cohort and summary of results

| Patient number | Age (years) | Sex | Histology | Treatment | Time between PET and MRI (days) | Tumour volume (mL) | Similarity coefficient | | Overlap volume (%) | FET vs. FLAIR | Tumour-to-brain ratio | | Extent of tumour resection | IDH genotype | MGMT promoter methylation | |
|----------------|-------------|-----|-----------|-----------|---------------------------------|--------------------|--------------------------|---------|--------------------|---------------|--------------------------|-----|----------------------------|--------------|---------------------------|--------------|
| | | | | | | | Dice | Jaccard | | | Mean | Max | | | | |
| | | | | | | On FET PET | On contrast-enhanced MRI | | | | | | | | | |
| 1 | 75 | m | GBM | None | 0 | 43.4 | 44.6 | 0.51 | 0.35 | 52 | FET < FLAIR | 1.9 | 3.3 | PR | wt | Unmethylated |
| 2 | 71 | f | GBM | None | 14 | 40.5 | 28.1 | 0.47 | 0.31 | 57 | FET < FLAIR ^a | 2.0 | 3.8 | PR | wt | Methylated |
| 3 | 58 | m | GBM | None | 0 | 32.8 | 16.5 | 0.65 | 0.48 | 96 | FET < FLAIR | 2.3 | 4.4 | PR | wt | Methylated |
| 4 | 78 | m | GBM | None | 1 | 14.0 | 21.9 | 0.16 | 0.09 | 20 | FET < FLAIR ^a | 1.8 | 2.6 | CR | wt | Unmethylated |
| 5 | 59 | m | GBM | None | 0 | 16.9 | 6.9 | 0.56 | 0.39 | 97 | FET = FLAIR | 2.7 | 5.7 | PR | wt | Unmethylated |
| 6 | 42 | f | GBM | None | 0 | 31.0 | 11.3 | 0.45 | 0.29 | 82 | FET < FLAIR | 1.9 | 3.7 | PR | wt | Unmethylated |
| 7 | 32 | f | GBM | None | 9 | 6.1 | 2.1 | 0.47 | 0.31 | 94 | FET < FLAIR | 2.8 | 8.7 | CR | wt | Methylated |
| 8 | 66 | m | GBM | None | 10 | 28.7 | 29.5 | 0.70 | 0.54 | 71 | FET = FLAIR | 2.2 | 4.0 | PR | wt | Unmethylated |
| 9 | 50 | m | GBM | None | 0 | 21.4 | 6.0 | 0.39 | 0.24 | 89 | FET < FLAIR | 2.2 | 4.0 | CR | wt | Unmethylated |
| 10 | 73 | f | GBM | None | 0 | 49.6 | 25.2 | 0.65 | 0.48 | 97 | FET < FLAIR | 3.3 | 8.3 | CR | wt | Unmethylated |
| 11 | 67 | f | GBM | None | 6 | 28.4 | 10.9 | 0.46 | 0.30 | 82 | FET < FLAIR | 2.1 | 3.3 | CR | wt | Unmethylated |
| 12 | 31 | m | GBM | None | 0 | 34.9 | 15.8 | 0.22 | 0.13 | 36 | FET < FLAIR | 2.0 | 3.6 | CR | mut | Methylated |
| 13 | 64 | f | GBM | None | 7 | 47.6 | 41.9 | 0.22 | 0.13 | 24 | FET < FLAIR | 2.0 | 3.8 | PR | wt | Methylated |
| 14 | 68 | m | GBM | None | 0 | 30.4 | 15.2 | 0.58 | 0.41 | 87 | FET < FLAIR | 2.5 | 4.9 | CR | n.a. | Methylated |
| 15 | 54 | m | GBM | None | 0 | 21.1 | 10.6 | 0.65 | 0.48 | 96 | FET < FLAIR | 2.5 | 4.5 | CR | wt | Unmethylated |
| 16 | 50 | f | GBM | None | 0 | 40.7 | 19.0 | 0.60 | 0.43 | 94 | FET = FLAIR | 2.6 | 5.6 | CR | wt | Unmethylated |
| 17 | 40 | m | GBM | None | 0 | 41.3 | 14.7 | 0.28 | 0.16 | 53 | FET = FLAIR | 2.4 | 5.4 | CR | mut | Methylated |
| 18 | 75 | m | GBM | None | 7 | 17.2 | 6.6 | 0.41 | 0.26 | 75 | – | 2.3 | 4.6 | CR | wt | Unmethylated |
| 19 | 49 | m | GBM | None | 17 | 15.1 | 0.9 | 0.11 | 0.06 | 0 | – | 2.8 | 6.8 | CR | wt | Methylated |
| 20 | 56 | f | GBM | None | 0 | 30.3 | 12.6 | 0.58 | 0.40 | 98 | FET < FLAIR | 2.6 | 4.6 | PR | mut | Methylated |
| 21 | 60 | m | GBM | None | 11 | 15.4 | 3.3 | 0.35 | 0.21 | 0 | FET = FLAIR | 2.5 | 4.1 | CR | wt | Unmethylated |
| 22 | 79 | m | GBM | None | 0 | 6.4 | 14.2 | 0.05 | 0.02 | 8 | FET < FLAIR | 1.2 | 2.8 | PR | n.a. | Unmethylated |
| 23 | 75 | m | GBM | None | 4 | 13.3 | 5.1 | 0.52 | 0.35 | 93 | FET < FLAIR | 2.5 | 4.7 | PR | wt | Unmethylated |

Table 1 (continued)

| Patient number | Age (years) | Sex | Histology | Treatment | Time between PET and MRI (days) | Tumour volume (mL) | | Similarity coefficient | | Overlap volume (%) | FET vs. FLAIR | Tumour-to-brain ratio | Extent of tumour resection | | IDH genotype | MGMT promoter methylation |
|----------------|-------------|-----|-----------|-----------|---------------------------------|--------------------|--------------------------|------------------------|---------|--------------------|--------------------------|-----------------------|----------------------------|-----|--------------|---------------------------|
| | | | | | | On FET PET | On contrast-enhanced MRI | Dice | Jaccard | | | | Mean | Max | | |
| 24 | 45 | m | GBM | None | 20 | 25.4 | 9.8 | 0.55 | 0.38 | 98 | FET < FLAIR | 3.1 | 6.4 | CR | wt | Unmethylated |
| 25 | 34 | m | GBM | None | 0 | 40.3 | 18.3 | 0.51 | 0.34 | 81 | FET < FLAIR | 2.0 | 3.3 | CR | n.a. | Methylated |
| 26 | 54 | m | GBM | None | 0 | 2.3 | 0.4 | 0.31 | 0.18 | 96 | FET < FLAIR | 1.9 | 2.9 | CR | wt | Methylated |
| 27 | 48 | f | GBM | None | 0 | 22.4 | 5.6 | 0.38 | 0.24 | 95 | FET < FLAIR | 2.5 | 5.1 | PR | wt | Unmethylated |
| 28 | 67 | f | GBM | None | 0 | 14.3 | 0.5 | 0.06 | 0.03 | 89 | FET = FLAIR | 2.3 | 4.1 | CR | n.a. | Unmethylated |
| 29 | 41 | f | GBM | None | 14 | 31.0 | 0.6 | 0.02 | 0.01 | 44 | FET < FLAIR | 2.0 | 3.2 | B | n.a. | Methylated |
| 30 | 50 | f | GBM | None | 10 | 2.8 | 0.0 | – | – | – | FET < FLAIR | 2.2 | 3.3 | CR | wt | Methylated |
| 31 | 66 | f | GBM | None | 30 | 28.1 | 0.0 | – | – | – | FET < FLAIR | 1.9 | 3.1 | B | wt | Methylated |
| 32 | 33 | f | GBM | None | 6 | 15.2 | 0.2 | 0.02 | 0.01 | 0 | – | 2.5 | 5.2 | CR | wt | Unmethylated |
| 33 | 66 | m | GBM | None | 7 | 10.0 | 1.7 | 0.27 | 0.16 | 94 | FET < FLAIR | 2.2 | 3.3 | B | wt | Methylated |
| 34 | 50 | m | GBM | None | 0 | 5.1 | 11.4 | 0.21 | 0.12 | 34 | FET < FLAIR | 1.7 | 2.7 | B | n.a. | methylated |
| 35 | 39 | m | GBM | None | 0 | 25.0 | 0.9 | 0.07 | 0.04 | 97 | FET > FLAIR ^a | 2.2 | 5.2 | PR | wt | Unmethylated |
| 36 | 55 | m | GBM | None | 0 | 26.9 | 7.1 | 0.41 | 0.26 | 95 | FET < FLAIR | 2.5 | 5.2 | PR | wt | Unmethylated |
| 37 | 51 | f | GBM | None | 11 | 7.5 | 0.0 | – | – | – | FET = FLAIR | 2.1 | 2.9 | CR | mut | Methylated |
| 38 | 59 | m | GBM | None | 0 | 0.7 | 0.0 | – | – | – | FET < FLAIR | 1.8 | 2.3 | CR | wt | Methylated |
| 39 | 59 | m | GBM | None | 0 | 5.5 | 0.0 | – | – | – | FET < FLAIR | 1.9 | 3.0 | CR | wt | Unmethylated |
| 40 | 66 | m | GBM | None | 7 | 56.4 | 0.0 | – | – | – | FET < FLAIR ^a | 2.5 | 4.6 | CR | wt | Unmethylated |
| 41 | 65 | m | GBM | None | 0 | 3.2 | 1.9 | 0.69 | 0.53 | 93 | FET < FLAIR ^a | 2.4 | 4.3 | CR | wt | Unmethylated |
| 42 | 55 | m | GBM | None | 0 | 22.0 | 0.0 | – | – | – | FET < FLAIR | 2.0 | 3.5 | B | wt | Unmethylated |
| 43 | 26 | f | GBM | None | 13 | 3.5 | 0.0 | – | – | – | FET < FLAIR | 1.7 | 2.1 | CR | wt | Methylated |
| 44 | 33 | m | GBM | None | 0 | 15.8 | 1.3 | 0.11 | 0.06 | 75 | FET < FLAIR | 2.0 | 3.2 | PR | mut | Methylated |

Table 1 (continued)

| Patient number | Age (years) | Sex | Histology | Treatment | Time between PET and MRI (days) | Tumour volume (mL) | | Similarity coefficient | Overlap volume (%) | FET vs. FLAIR | Tumour-to-brain ratio | | Extent of tumour resection | IDH genotype | MGMT promoter methylation |
|----------------|-------------|-----|-----------|-----------|---------------------------------|--------------------|--------------------------|------------------------|--------------------|---------------|-----------------------|-----|----------------------------|--------------|---------------------------|
| | | | | | | On PET | On contrast-enhanced MRI | | | | Mean | Max | | | |
| 45 | 72 | m | GBM | None | 8 | 4.8 | 4.4 | 0.67 | 70 | FET < FLAIR | 2.2 | 3.6 | B | wt | Unmethylated |
| 46 | 57 | m | GBM | None | 0 | 12.2 | 1.8 | 0.23 | 92 | FET = FLAIR | 2.3 | 5.0 | B | wt | Unmethylated |
| 47 | 78 | f | GBM | None | 7 | 15.1 | 31.9 | 0.34 | 53 | FET = FLAIR | 1.8 | 2.6 | B | wt | Unmethylated |
| 48 | 57 | f | GBM | None | 1 | 1.4 | 0.7 | 0.58 | 91 | – | 2.1 | 3.6 | B | wt | Unmethylated |
| 49 | 67 | f | GBM | None | 9 | 29.7 | 0.0 | – | – | FET = FLAIR | 2.0 | 3.0 | B | wt | Unmethylated |
| 50 | 44 | m | GBM | None | 0 | 0.0 | 0.0 | – | – | FET < FLAIR | – | – | B | mut | Methylated |
| Mean | 56 | | | | 5 | 21.1 | 9.2 | 0.39 | 77 | FLAIR | 2.2 | 4.2 | | | |
| SD | 14 | | | | 7 | 14.5 | 11.2 | 0.21 | 26 | | 0.4 | 1.4 | | | |
| Min | 26 | | | | 0 | 0.0 | 0.0 | 0.02 | 8 | | 1.2 | 3.8 | | | |
| Max | 79 | | | | 30 | 56.4 | 44.6 | 0.70 | 100 | | 3.3 | 8.7 | | | |

B stereotactic biopsy, *CR* complete resection, *PR* partial resection, *GBM* glioblastoma, *IDH* isocitrate dehydrogenase, *MGMT O⁶*-methylguanine-DNA methyltransferase, *mut* mutant, *n.a.* not available, *wt* wild-type

^a FET partially outside FLAIR

Data analysis and calculation of tumour volumes

After adjusting the spatial resolution of the BrainPET images to those of the ECAT EXACT HR+ scanner by applying a 2.5 mm 3D gaussian filter [30], PET images were corrected for motion, and the MR and PET images (summation images from 20 to 40 min after injection) were resliced to a voxel size of $1 \times 1 \times 1$ mm using the software PMOD, version 3.505 (PMOD Technologies Ltd.) to provide robust coregistration and accurate volume calculations. MR and PET images were then coregistered using rigid matching algorithms from PMOD. The results of the coregistration process were validated visually and, if necessary, manual correction was performed according to anatomical landmarks. Areas of contrast enhancement on the T1-weighted MR images were manually segmented on each consecutive transverse slice, and the sum of the circumscribed areas was multiplied by the slice thickness to obtain volumes of interest (VOI) representing the total volume of contrast enhancement in each patient. Necrotic parts were excluded from the volume of contrast enhancement. A second investigator validated the results of coregistration and the manual delineation. Since most patients exhibited diffuse and widespread FLAIR hyperintensities, reproducible and objective segmentation was not possible.

Standardized uptake values (SUV) were used for normalization of FET uptake by dividing the radioactivity in the tissue by the radioactivity injected per gram of body weight. A spherical VOI of constant size (diameter 30 mm) was positioned in normal-appearing brain tissue including grey and white matter in the hemisphere contralateral to the lesion. A 3D autocontouring process using a tumour-to-brain ratio (TBR) of 1.6 or more was used for segmentation of the tumour volume. This threshold was based on a biopsy-controlled study in which this value provided the best separation between vital tumour and healthy brain parenchyma on FET PET [19]. Mean TBR (TBR_{mean}) was calculated by dividing the mean SUV of the tumour VOI by the mean SUV of the background VOI. The maximum TBR (TBR_{max}) was calculated by dividing the maximum SUV of the tumour VOI by the mean SUV of the background VOI.

Calculation of spatial correlation and overlap between MRI-based and PET-based tumour volumes

As a measure of spatial correlation [31], the spatial similarity between the VOIs defined by contrast enhancement on MRI and increased tracer uptake on FET PET was evaluated using the Dice similarity coefficient (DSC) [32] and the Jaccard similarity coefficient (JSC) [33]. The DSC is calculated as:

$$DSC(V_{\text{PET}}, V_{\text{MRI}}) = \frac{2(V_{\text{PET}} \cap V_{\text{MRI}})}{V_{\text{PET}} + V_{\text{MRI}}},$$

where V_{PET} and V_{MRI} are the VOIs defined by FET PET and MRI, respectively. The JSC is calculated as:

$$JSC(V_{\text{PET}}, V_{\text{MRI}}) = \frac{V_{\text{PET}} \cap V_{\text{MRI}}}{V_{\text{PET}} \cup V_{\text{MRI}}} = \frac{DSC}{2 - DSC},$$

which is the ratio of the intersection and the union of the FET PET and the MRI VOIs. Additionally, the overlap volume (OV) [31] was calculated. The OV considers, in contrast to the DSC and JSC, volumetric differences between the FET PET and MRI VOIs, and is defined as the ratio of the intersection and the smallest volume according to:

$$OV(V_{\text{PET}}, V_{\text{MRI}}) = \frac{V_{\text{PET}} \cap V_{\text{MRI}}}{\min(V_{\text{PET}}, V_{\text{MRI}})}.$$

While DSC and JSC are similarity coefficients that range between 0 (no similarity) and 1 (perfect agreement), the OV is an overlap coefficient with a value of 100% indicating that one volume is completely contained within the other. All calculations were implemented and performed in MATLAB, version R2015a (Mathworks, Inc.). Figure 1 shows the differences between the three coefficients.

Visual analysis of spatial correlation between FET-based and FLAIR-based tumour volumes

The spatial correlation between FET-based and FLAIR-based tumour volumes was assessed visually according to the following criteria: (1) FET-based tumour volume larger than FLAIR-based tumour volume, (2) FET-based tumour volume smaller than FLAIR-based tumour volume, (3) FET-based tumour volume similar to FLAIR-based tumour volume, and (4) FET-based tumour volume partially located outside FLAIR-based tumour volume. The results of the visual analysis were validated by a second investigator.

Statistical analysis

Descriptive statistics are presented as means and standard deviations or medians and ranges. The nonparametric Wilcoxon rank-sum test was used for intergroup comparisons. *P* values less than 0.05 were considered significant. Statistical analysis was performed using the statistical software packages SPSS, version 24 (IBM Corp.) and Excel (Excel for Mac 2016, version 16.12; Microsoft Corp.).

Results

Tumour volumes

One patient showed neither FET uptake nor contrast enhancement. All the remaining 49 patients showed increased FET

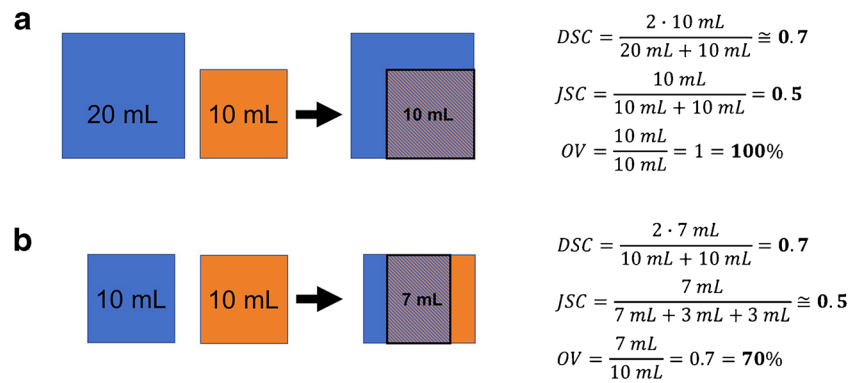


Fig. 1 Relationships between the Dice similarity coefficient (DSC), Jaccard similarity coefficient (JSC), and the overlap volume (OV). Similarity coefficients are commonly used for comparing algorithms for image segmentation against a known reference mask (ground truth). To find out the volume differences between two different imaging modalities, e.g. FET PET and contrast enhancement, the ground truth (true tumour extent) is usually not known. Thus, the results from similarity coefficients can be misleading and have to be interpreted with

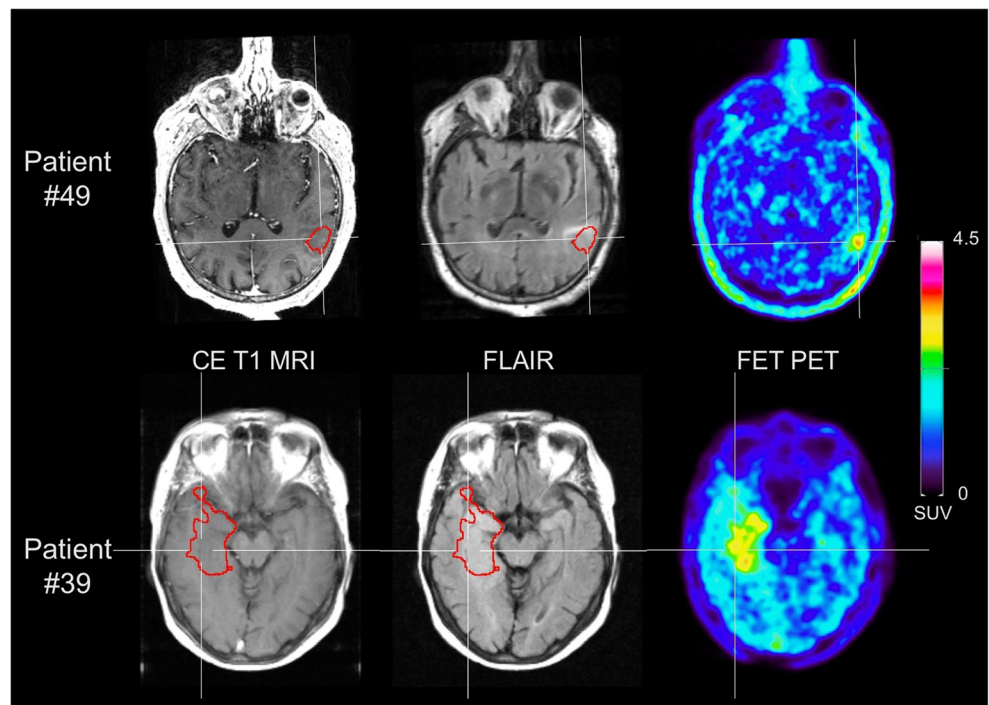
caution. **a** Two volumes of different size (20 mL, 10 mL) completely overlap. **b** Two volumes of equal size (10 mL) only partially overlap. Nevertheless, the similarity coefficients DSC and JSC yield identical results in both cases (DSC 0.7, JSC 0.5), indicating the same spatial similarity. On the other hand, the measure OV depends on the volume and gives different results between the two cases (**a** OV 100%, **b** OV 70%). Therefore, the combination of OV with DSC and JSC allows improved interpretation of volumetric properties

uptake (average $TBR_{\text{mean}} 2.2 \pm 0.4$, range 1.2–3.3; average $TBR_{\text{max}} 4.2 \pm 1.4$, range 2.1–8.7). Ten patients (20%) showed no contrast enhancement on MRI (Fig. 2). The FET PET tumour volumes and the contrast enhancement volumes were in the range 0.0–56.4 mL and 0.0–44.6 mL, respectively. In 43 patients (86%), the average FET PET tumour volume was significantly larger than the average contrast enhancement volume ($21.5 \pm 14.3 \text{ mL}$ vs. $9.4 \pm 11.3 \text{ mL}$; $P < 0.001$). These results are summarized in Table 1 and Fig. 3.

Overlap and spatial similarity between MRI-based and PET-based tumour volumes

Of the 50 patients, 40 (80%) showed increases in both FET uptake and contrast enhancement on MRI. In these 40 patients, the OV was moderate (mean $OV 77 \pm 26\%$, range 8–100%), but the spatial similarity was low (mean $DSC 0.39 \pm 0.21$, range 0.02–0.70; mean $JSC 0.26 \pm 0.16$, range 0.01–0.54). Furthermore, 6 of these 40 patients (15%)

Fig. 2 Contrast-enhanced (CE) MR images (left), fluid-attenuated inversion recovery (FLAIR) MR images (centre) and FET PET images (right) in representative patients without contrast enhancement (patients 49 and 39). The tumour volume segmented by FET PET based on a tumour-to-brain ratio of more than 1.6 is projected onto the MR images (red contour). A considerable portion of FET PET tumour volume is located outside the FLAIR hyperintensity in patient 49 (top). In general, there are considerable discrepancies among the CE MRI, FLAIR and FET PET images



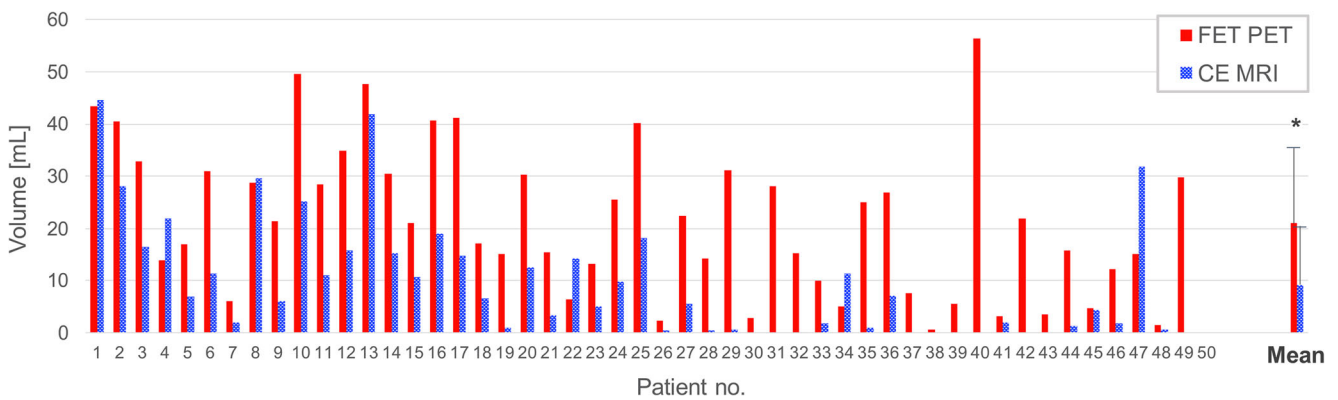


Fig. 3 Differences between FET PET tumour volumes (*red*) and contrast-enhanced MRI tumour volumes (*blue*). In ten patients (20%), no contrast enhancement was present. In 43 patients (86%), the FET PET volume is

considerably larger than the respective contrast enhancement MRI volume. * $P < 0.001$

showed both a low OV of less than 50% (mean OV $28 \pm 15\%$) as well as a low spatial similarity (mean DSC 0.15 ± 0.08 , mean JSC 0.08 ± 0.05). In total, 16 patients (32%) showed either no contrast enhancement (Fig. 2) or an OV of $<50\%$ in combination with a low spatial similarity (DSC <0.4 , JSC <0.3).

Overlap and spatial similarity depending on tumour volume

In a subgroup analysis, 6 of 50 patients (12%) with a FET PET tumour volume smaller than the contrast enhancement volume showed both a low OV (mean OV $40 \pm 21\%$, range 8–71%) and low spatial similarity (mean DSC 0.33 ± 0.24 , range 0.05–0.70; mean JSC 0.22 ± 0.19 , range 0.02–0.54). Patients with a FET PET tumour volume larger than the contrast enhancement volume ($n = 43$) had a high OV (mean OV $84 \pm 20\%$, range 24–100%) but a low spatial similarity (mean DSC 0.40 ± 0.24 , range 0.02–0.69; mean JSC 0.27 ± 0.18 , range 0.01–0.53). These results are summarized in Table 1 and Fig. 3. Figure 4 shows contrast-enhanced MRI and FET PET tumour volumes and their overlap in two representative patients.

Spatial correlation of PET-based and FLAIR-based tumour volumes

The FET PET tumour volume was clearly smaller than the FLAIR volume in 35 patients (70%). In ten patients (20%), the FET PET volume was similar to the FLAIR volume and in one patient (2%) the FET PET volume was larger than the FLAIR volume. In five patients (10%), a considerable portion of the FET PET tumour volume was outside the FLAIR volume (Fig. 2, top row). These results are summarized in Table 1.

Discussion

Using MRI and amino acid PET, previous studies have compared predominantly tumour volumes. To the best of our knowledge, this study is the first in this group of patients that has assessed and evaluated various volumetric parameters. The main finding of our study is that there were significant differences in size, overlap and spatial correlation of tumour volumes, indicating that conventional contrast-enhanced MRI substantially underestimates tumour volume. In 43 of the 50 patients (86%) the FET PET tumour volume was significantly larger than the contrast enhancement volume. Interestingly, ten of the 50 patients (20%) showed no contrast enhancement. One of these patients additionally showed no FET uptake. Furthermore, in the remaining 40 patients (80%) with increased FET uptake and contrast enhancement, the spatial similarity (evaluated using the DSC and JSC) was low despite moderate OV (average OV, 77%). Moreover, in six of these 40 patients (15%), the spatial similarity between the FET PET volume and the contrast enhancement volume was low and the OV was $<50\%$, i.e. relevant FET PET volumes were located partially outside and hence extended beyond the contrast enhancement volumes (Fig. 4). In total, 16 of the 50 patients (32%) showed either no contrast enhancement at all or a low OV in combination with a low spatial similarity between the FET PET volume and the contrast enhancement volume.

The OV when applied alone needs to be interpreted with caution, i.e. a high OV represents only two spatially congruent volumes if both volumes are of similar size. If the volumes are different, the interpretation of the OV alone may be misleading. The addition of measures of spatial similarity such as the DSC and the JSC for combined interpretation of the results leads to a correct impression of the spatial orientation (Figs. 1 and 4). In the present study, the OV of nearly 80% between FET PET and contrast-enhanced MRI volumes in our patient cohort might have led to the premature conclusion that the contrast-enhanced MRI volume adequately represents the metabolically

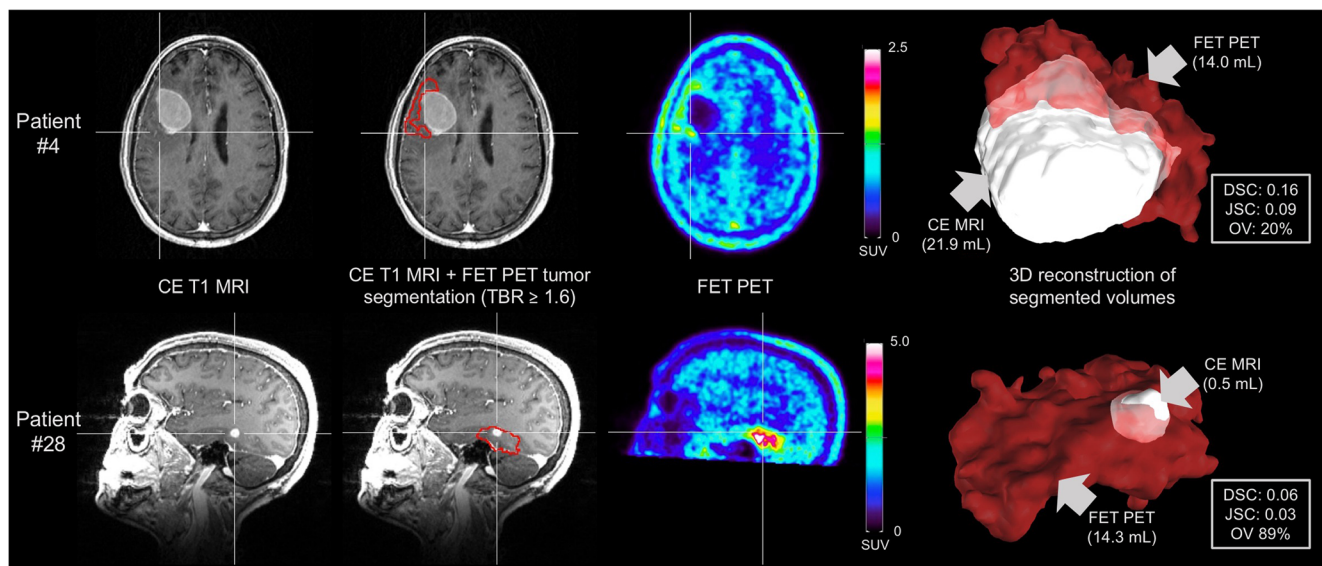


Fig. 4 Contrast-enhanced (CE) MR images (*left*), CE MR images with projection of the FET PET tumour volume segmentation using a tumour-to-brain ratio of 1.6 or more (*second column, red contour*), FET PET images (*third column*), and 3D reconstruction images of the segmented tumour volumes (*right*) based on CE MRI (*white*) and FET PET (*red*) in two representative patients. *Patient 4*: The contrast enhancement volume is larger than the FET uptake volume (21.9 mL vs. 14.0 mL). The area of FET uptake is partially outside and beyond the area of contrast

enhancement. The spatial similarity and the overlap volume are low (DSC 0.16, JSC 0.09, OV 20%). *Patient 28*: The contrast enhancement volume is smaller than the FET uptake volume (0.5 mL vs. 14.3 mL). The contrast enhancement volume is mainly contained within the FET PET volume. Despite a high overlap volume (OV 89%), the spatial similarity is low (DSC 0.06, JSC 0.03). In both examples, only combined interpretation of the overlap and spatial similarity measures leads to a correct impression of the spatial orientation

active tumour in the majority of patients. However, combined evaluation of OV and low spatial similarity (DSC <0.4, JSC <0.3) shows that a high OV is biased by the initial differences between the tumour volumes defined by contrast enhancement and increased FET uptake. These important differences between the volumetric measures used are illustrated in more detail in Figs. 1 and 4.

Visual analysis of the spatial similarity between FLAIR and FET PET tumour volumes revealed significant differences. Although the hyperintense areas on FLAIR images were larger than both the contrast enhancement areas and areas of increased FET uptake in 70% of patients, a considerable proportion of the tumour volume on FET PET was located outside the FLAIR signal in 10% of patients. Thus, even the combination of contrast enhancement and FLAIR hyperintensity did not cover the full extent of the tumour in all GBM patients (Fig. 2, top row).

The value of PET using the PET amino acid tracer MET in brain tumour assessment in comparison with conventional MRI has been investigated in several studies. For example, Pirotte et al. [34] found that a MET PET-guided “complete” tumour resection significantly prolonged overall survival in patients with high-grade glioma whereas “complete” resection based on contrast enhancement did not. Grosu et al. [35] investigated the value of MET PET in comparison with conventional MRI for target volume definition before radiotherapy in patients with resected high-grade glioma. In 74% of the patients, gross tumour volumes based on MET PET were considerably larger

than those based on contrast-enhanced MRI, a finding confirmed by Mahasittiwat et al. [36]. Assessing the spatial differences between MET PET and contrast-enhanced MRI tumour volumes in patients with recurrent GBM, we observed that contrast-enhanced MRI substantially underestimated the metabolically active tumour volume as defined on MET PET [24]. However, the short half-life of ^{11}C (20 min) restricts the use of MET to institutions with an on-site cyclotron.

The use of FET labelled with ^{18}F (half-life 110 min) overcomes the logistic disadvantages of MET. FET PET has been intensively evaluated over the last two decades for the detection of vital tumour tissue for biopsy guidance and treatment planning, especially for neurosurgical resection and radiotherapy [37]. Usually, summed images obtained from 20 to 40 min after injection are used for the analysis of FET PET scans in patients with brain tumours. Unterrainer et al. [38] recently reported that the FET PET tumour volume is considerably larger in early summation images obtained from 5 to 15 min after injection, especially in high-grade gliomas. Consequently, the true discrepancy between conventional MRI and FET PET tumour volumes might be even larger if early summation images are used for FET PET tumour segmentation. However, in that study validation by histological evaluation of local stereotactic biopsies to determine the true tumour extent was not performed.

Predominantly, the impact of FET PET on radiotherapy target volume definition in patients with low-grade and high-grade gliomas has been investigated [39–42]. These studies provide converging evidence that the spatial correlation

between MRI and FET PET target volumes is low and that FET PET target volumes are considerably larger than MRI target volumes. Consequently, the integration of FET PET for target volume definition has been recommended. However, these studies did not further investigate in detail the OV's or the spatial correlation using dedicated quantitative measures such as the DSC or JSC. To the best of our knowledge, only two studies have investigated the spatial similarity between FET PET and contrast enhancement tumour volumes using the DSC, in analogy to our study. Henriksen et al. [43] calculated the DSC between FET PET and contrast-enhanced MRI tumour volumes in 17 of 32 patients with pretreated low-grade and high-grade gliomas. The estimated spatial similarity was low (mean DSC 0.19) and only 8 of the 17 patients had a DSC of more than 0.1. In our study, the spatial similarity was higher (mean DSC 0.39) and only five patients had a DSC below 0.1, most likely because of a more homogeneous patient population. Henriksen et al. also found that the metabolic tumour volume as delineated using a TBR of more than 1.6 (i.e. identical to our approach) was significantly larger than the contrast enhancement volume, which is in line with our results. However, the number of patients in that study was small, and the patient population was comparatively heterogeneous (5 patients with low-grade glioma and 12 patients with high-grade glioma), which is also reflected in the variety of pre-treatments including antiangiogenic therapy.

Unterrainer et al. [44] also calculated the DSC between FET PET and contrast-enhanced MRI tumour volumes in 20 patients with high-grade glioma at initial diagnosis or recurrence prior to any further therapy. The mean DSC was 0.38, which is in good agreement with our results (mean DSC, 0.39).

Considering that a maximally safe tumour resection is a critical component in the treatment of patients with GBM due to its survival benefits, adequate preoperative volumetric representation of the metabolically active tumour tissue is especially important. There is substantial evidence in the literature that the extent of tumour resection is a prognostic factor in patients with glioma [4, 8, 9, 45]. Consequently, correct preoperative spatial delineation of the vital tumour tissue is essential for maximizing the extent of resection. In many centres, 5-aminolevulinic acid (5-ALA) fluorescence is used intraoperatively to identify tumour tissue [4]. It has been demonstrated that a 5-ALA fluorescence-guided tumour resection in patients with GBM is associated with improved progression-free survival at 6 months [4]. In that study, it was also demonstrated that 5-ALA fluorescence identifies tumour tissue beyond areas of preoperative MRI contrast enhancement, indicating that 5-ALA fluorescence delineates nonenhancing parts of the tumour. This confirms the low sensitivity of MRI in correctly representing tumour tissue [46]. It is noteworthy that FET PET has been found to be even more sensitive in detecting glioma tissue than 5-ALA fluorescence [47].

A limitation of our study was the lack of confirmation of the spatial neuroimaging findings by histological evaluation

of local stereotactic biopsies. Thus, prospective studies including spatial correlation between imaging findings and histological findings in stereotactic biopsies are needed to confirm our results. On the other hand, the patient cohort was fairly homogeneous (i.e. in all patients, GBM was confirmed neuropathologically according to the 2016 WHO classification of brain tumours [48]) and all tumours were untreated. Furthermore, three different quantitative measures to describe the spatial similarity and OV were used to assess volumetric and spatial differences between the FET PET and contrast enhancement tumour volumes. Furthermore, spatial differences between areas of FLAIR hyperintensity and FET PET tumour volume were evaluated visually.

In conclusion, our results suggest that the metabolically active tumour volume in patients with newly diagnosed, untreated GBM is critically underestimated by contrast-enhanced MRI. Furthermore, the spatial similarity between the contrast-enhanced MRI and FET PET tumour volumes was low, i.e. the areas of FET uptake extended substantially beyond the area of contrast enhancement and also beyond the area of FLAIR hyperintensity in some patients. In these patients, FET PET yields essential information for correct tumour delineation beyond the area of contrast enhancement and thereby contributes significantly to tailoring the tumour resection. It remains to be determined whether FET PET-guided tumour resection or target volume delineation before radiotherapy significantly affects patient survival. A randomized phase II trial (NOA-10/GLIAA study) [49] is currently evaluating whether radiotherapy target volume delineation by amino acid PET significantly prolongs survival in comparison with contrast-enhanced MRI in patients with progressive GBM.

Acknowledgments The authors thank Suzanne Schaden, Trude Plum, Natalie Judov, Silke Frensch, Kornelia Frey and Lutz Tellmann for assistance with the patient studies, and Johannes Ernert, Silke Grafmüller, Erika Wabbals and Sascha Rehbein for radiosynthesis of FET.

Funding This study was funded by Wilhelm Sander-Stiftung, Munich, Germany (grant number 2016.069.1 to N.G.)

Compliance with ethical standards

Conflicts of interest None.

Ethical approval All procedures performed in studies involving human participants were in accordance with the ethical standards of the institutional and/or national research committee and with the principles of the 1964 Declaration of Helsinki and its later amendments or comparable ethical standards. For this type of study formal consent is not required.

Informed consent Informed consent was obtained from all individual participants included in the study.

References

- Stupp R, Mason WP, van den Bent MJ, Weller M, Fisher B, Taphoorn MJ, et al. Radiotherapy plus concomitant and adjuvant temozolomide for glioblastoma. *N Engl J Med*. 2005;352(10):987–96.
- Chinot OL, Wick W, Mason W, Henriksson R, Saran F, Nishikawa R, et al. Bevacizumab plus radiotherapy-temozolomide for newly diagnosed glioblastoma. *N Engl J Med*. 2014;370(8):709–22.
- Weller M, Butowski N, Tran DD, Recht LD, Lim M, Hirte H, et al. Rindopemimut with temozolomide for patients with newly diagnosed, EGFRvIII-expressing glioblastoma (ACT IV): a randomised, double-blind, international phase 3 trial. *Lancet Oncol*. 2017;18(10):1373–85.
- Stummer W, Pichlmeier U, Meinel T, Wiestler OD, Zanella F, Reulen HJ, et al. Fluorescence-guided surgery with 5-aminolevulinic acid for resection of malignant glioma: a randomised controlled multicentre phase III trial. *Lancet Oncol*. 2006;7(5):392–401.
- Albert FK, Forsting M, Sartor K, Adams HP, Kunze S. Early post-operative magnetic resonance imaging after resection of malignant glioma: objective evaluation of residual tumor and its influence on regrowth and prognosis. *Neurosurgery*. 1994;34(1):45–60.
- Aghi MK, Nahed BV, Sloan AE, Ryken TC, Kalkanis SN, Olson JJ. The role of surgery in the management of patients with diffuse low grade glioma: a systematic review and evidence-based clinical practice guideline. *J Neurooncol*. 2015;125(3):503–30.
- Brown TJ, Brennan MC, Li M, Church EW, Brandmeir NJ, Rakszawski KL, et al. Association of the extent of resection with survival in glioblastoma: a systematic review and meta-analysis. *JAMA Oncol*. 2016;2(11):1460–9.
- Kreth FW, Thon N, Simon M, Westphal M, Schackert G, Ninkkrah G, et al. Gross total but not incomplete resection of glioblastoma prolongs survival in the era of radiochemotherapy. *Ann Oncol*. 2013;24(12):3117–23.
- Lacroix M, Abi-Said D, Fourney DR, Gokaslan ZL, Shi W, DeMonte F, et al. A multivariate analysis of 416 patients with glioblastoma multiforme: prognosis, extent of resection, and survival. *J Neurosurg*. 2001;95(2):190–8.
- Niyazi M, Brada M, Chalmers AJ, Combs SE, Erridge SC, Fiorentino A, et al. ESTRO-ACROP guideline "target delineation of glioblastomas". *Radiother Oncol*. 2016;118(1):35–42.
- Halperin EC, Bentel G, Heinz ER, Burger PC. Radiation therapy treatment planning in supratentorial glioblastoma multiforme: an analysis based on post mortem topographic anatomy with CT correlations. *Int J Radiat Oncol Biol Phys*. 1989;17(6):1347–50.
- Lunsford LD, Martinez AJ, Latchaw RE. Magnetic resonance imaging does not define tumor boundaries. *Acta Radiol Suppl*. 1986;369:154–6.
- Eidel O, Burth S, Neumann JO, Kieslich PJ, Sahn F, Jungk C, et al. Tumor infiltration in enhancing and non-enhancing parts of glioblastoma: a correlation with histopathology. *PLoS One*. 2017;12(1):e0169292.
- Tovi M, Hartman M, Lilja A, Ericsson A. MR imaging in cerebral gliomas. *Acta Radiol*. 1994;35(5):495–505.
- Ginsberg LE, Fuller GN, Hashmi M, Leeds NE, Schomer DF. The significance of lack of MR contrast enhancement of supratentorial brain tumors in adults: histopathological evaluation of a series. *Surg Neurol*. 1998;49(4):436–40.
- Rapp M, Heinzel A, Galldiks N, Stoffels G, Felsberg J, Ewelt C, et al. Diagnostic performance of 18F-FET PET in newly diagnosed cerebral lesions suggestive of glioma. *J Nucl Med*. 2013;54(2):229–35.
- Hutterer M, Nowosielski M, Putzer D, Jansen NL, Seiz M, Schocke M, et al. [18F]-fluoro-ethyl-L-tyrosine PET: a valuable diagnostic tool in neuro-oncology, but not all that glitters is glioma. *Neuro Oncol*. 2013;15(3):341–51.
- Weller M, van den Bent M, Tonn JC, Stupp R, Preusser M, Cohen-Jonathan-Moyal E, et al. European Association for Neuro-Oncology (EANO) guideline on the diagnosis and treatment of adult astrocytic and oligodendroglial gliomas. *Lancet Oncol*. 2017;18(6):e315–29.
- Pauleit D, Floeth F, Hamacher K, Riemenschneider MJ, Reifenberger G, Muller HW, et al. O-(2-[18F]fluoroethyl)-L-tyrosine PET combined with MRI improves the diagnostic assessment of cerebral gliomas. *Brain*. 2005;128(Pt 3):678–87.
- Galldiks N, Stoffels G, Filss C, Rapp M, Blau T, Tscherpel C, et al. The use of dynamic O-(2-18F-fluoroethyl)-l-tyrosine PET in the diagnosis of patients with progressive and recurrent glioma. *Neuro Oncol*. 2015;17(9):1293–300.
- Jansen NL, Suchorska B, Wenter V, Schmid-Tannwald C, Todica A, Eigenbrod S, et al. Prognostic significance of dynamic 18F-FET PET in newly diagnosed astrocytic high-grade glioma. *J Nucl Med*. 2015;56(1):9–15.
- Albert NL, Weller M, Suchorska B, Galldiks N, Soffietti R, Kim MM, et al. Response Assessment in Neuro-Oncology working group and European Association for Neuro-Oncology recommendations for the clinical use of PET imaging in gliomas. *Neuro Oncol*. 2016;18(9):1199–208.
- Pirotte B, Goldman S, Massager N, David P, Wikler D, Vandesteene A, et al. Comparison of 18F-FDG and 11C-methionine for PET-guided stereotactic brain biopsy of gliomas. *J Nucl Med*. 2004;45(8):1293–8.
- Galldiks N, Ullrich R, Schroeter M, Fink GR, Jacobs AH, Kracht LW. Volumetry of [(11)C]-methionine PET uptake and MRI contrast enhancement in patients with recurrent glioblastoma multiforme. *Eur J Nucl Med Mol Imaging*. 2010;37(1):84–92.
- Mosskin M, Ericson K, Hindmarsh T, Vonholst H, Collins VP, Bergstrom M, et al. Positron emission tomography compared with magnetic-resonance imaging and computed-tomography in supratentorial gliomas using multiple stereotactic biopsies as reference. *Acta Radiol*. 1989;30(3):225–32.
- Bergström M, Collins VP, Ehrin E, Ericson K, Eriksson L, Greitz T, et al. Discrepancies in brain tumor extent as shown by computed tomography and positron emission tomography using [68Ga]EDTA, [11C]glucose, and [11C]methionine. *J Comput Assist Tomogr*. 1983;7(6):1062–6.
- Hamacher K, Coenen HH. Efficient routine production of the 18F-labelled amino acid O-2-18F fluoroethyl-L-tyrosine. *Appl Radiat Isot*. 2002;57(6):853–6.
- Langen KJ, Bartenstein P, Boecker H, Brust P, Coenen HH, Drzezga A, et al. German guidelines for brain tumour imaging by PET and SPECT using labelled amino acids. *Nuklearmedizin*. 2011;50(4):167–73.
- Kops ER, Herzog H. Template based attenuation correction for PET in MR-PET scanners. *IEEE Nuclear Science Symposium Conference Record*. 2008. p. 3786–9.
- Lohmann P, Herzog H, Rota Kops E, Stoffels G, Judov N, Filss C, et al. Dual-time-point O-(2-[(18)F]fluoroethyl)-L-tyrosine PET for grading of cerebral gliomas. *Eur Radiol*. 2015;25(10):3017–24.
- Besemer AE, Titz B, Grudzinski JJ, Weichert JP, Kuo JS, Robins HI, et al. Impact of PET and MRI threshold-based tumor volume segmentation on patient-specific targeted radionuclide therapy dosimetry using CLR1404. *Phys Med Biol*. 2017;62(15):6008–25.
- Dice LR. Measures of the amount of ecologic association between species. *Ecology*. 1945;26(3):297–302.
- Jaccard P. The distribution of the flora in the alpine zone. *New Phytol*. 1912;11(2):37–50.
- Pirotte BJ, Levivier M, Goldman S, Massager N, Wikler D, Dewitte O, et al. Positron emission tomography-guided volumetric resection

- of supratentorial high-grade gliomas: a survival analysis in 66 consecutive patients. *Neurosurgery*. 2009;64(3):471–81.
35. Grosu AL, Weber WA, Riedel E, Jeremic B, Nieder C, Franz M, et al. L-(methyl-11C) methionine positron emission tomography for target delineation in resected high-grade gliomas before radiotherapy. *Int J Radiat Oncol Biol Phys*. 2005;63(1):64–74.
 36. Mahasittiwat P, Mizoe JE, Hasegawa A, Ishikawa H, Yoshikawa K, Mizuno H, et al. l-[METHYL-(11)C] methionine positron emission tomography for target delineation in malignant gliomas: impact on results of carbon ion radiotherapy. *Int J Radiat Oncol Biol Phys*. 2008;70(2):515–22.
 37. Misch M, Guggemos A, Driever PH, Koch A, Grosse F, Steffen IG, et al. (18)F-FET-PET guided surgical biopsy and resection in children and adolescence with brain tumors. *Childs Nerv Syst*. 2015;31(2):261–7.
 38. Unterrainer M, Winkelmann I, Suchorska B, Giese A, Wenter V, Kreth FW, et al. Biological tumour volumes of gliomas in early and standard 20–40 min (18)F-FET PET images differ according to IDH mutation status. *Eur J Nucl Med Mol Imaging*. 2018;45(7):1242–9.
 39. Rieken S, Habermehl D, Giesel FL, Hoffmann C, Burger U, Rief H, et al. Analysis of FET-PET imaging for target volume definition in patients with gliomas treated with conformal radiotherapy. *Radiother Oncol*. 2013;109(3):487–92.
 40. Niyazi M, Geisler J, Siefert A, Schwarz SB, Ganswindt U, Garny S, et al. FET-PET for malignant glioma treatment planning. *Radiother Oncol*. 2011;99(1):44–8.
 41. Jaymanne DT, Kaushal S, Chan D, Schembri G, Brazier D, Bailey D, et al. Utilizing 18F-fluoroethyl-l-tyrosine positron emission tomography in high grade glioma for radiation treatment planning in patients with contraindications to MRI. *J Med Imaging Radiat Oncol*. 2018;62(1):122–7.
 42. Debus C, Waltenberger M, Floca R, Afshar-Oromieh A, Bougatf N, Adeberg S, et al. Impact of (18)F-FET PET on target volume definition and tumor progression of recurrent high grade glioma treated with carbon-ion radiotherapy. *Sci Rep*. 2018;8(1):7201.
 43. Henriksen OM, Larsen VA, Muhic A, Hansen AE, Larsson HB, Poulsen HS, et al. Simultaneous evaluation of brain tumour metabolism, structure and blood volume using [(18)F]-fluoroethyltyrosine (FET) PET/MRI: feasibility, agreement and initial experience. *Eur J Nucl Med Mol Imaging*. 2016;43(1):103–12.
 44. Unterrainer M, Fleischmann DF, Diekmann C, Vomacka L, Lindner S, Vettermann F, et al. Comparison of (18)F-GE-180 and dynamic (18)F-FET PET in high grade glioma: a double-tracer pilot study. *Eur J Nucl Med Mol Imaging*. 2018. <https://doi.org/10.1007/s00259-018-4166-1>
 45. Sanai N, Polley MY, McDermott MW, Parsa AT, Berger MS. An extent of resection threshold for newly diagnosed glioblastomas. *J Neurosurg*. 2011;115(1):3–8.
 46. Schucht P, Knittel S, Slotboom J, Seidel K, Murek M, Jilch A, et al. 5-ALA complete resections go beyond MR contrast enhancement: shift corrected volumetric analysis of the extent of resection in surgery for glioblastoma. *Acta Neurochir*. 2014;156(2):305–12.
 47. Floeth FW, Sabel M, Ewelt C, Stummer W, Felsberg J, Reifenberger G, et al. Comparison of (18)F-FET PET and 5-ALA fluorescence in cerebral gliomas. *Eur J Nucl Med Mol Imaging*. 2011;38(4):731–41.
 48. Louis DN, Perry A, Reifenberger G, von Deimling A, Figarella-Branger D, Cavenee WK, et al. The 2016 World Health Organization classification of tumors of the central nervous system: a summary. *Acta Neuropathol*. 2016;131(6):1–18.
 49. Oehlke O, Mix M, Graf E, Schimek-Jasch T, Nestle U, Gotz I, et al. Amino-acid PET versus MRI guided re-irradiation in patients with recurrent glioblastoma multiforme (GLIAA) – protocol of a randomized phase II trial (NOA 10/ARO 2013-1). *BMC Cancer*. 2016;16(1):769.